

Galaxy spin as a formation probe: the stellar-to-halo specific angular momentum relation

Lorenzo Posti^{1*}, Gabriele Pezzulli², Filippo Fraternali^{3,1} and Enrico M. Di Teodoro⁴

¹*Kapteyn Astronomical Institute, University of Groningen, P.O. Box 800, 9700 AV Groningen, the Netherlands*

²*Department of Physics, ETH Zurich, Wolfgang-Pauli-Strasse 27, 8093 Zurich, Switzerland*

³*Dipartimento di Fisica e Astronomia, Università di Bologna, via Gobetti 93/2, I-40129 Bologna, Italy*

⁴*Research School of Astronomy and Astrophysics - The Australian National University, Canberra, ACT, 2611, Australia*

December 5th 2017

ABSTRACT

We derive the stellar-to-halo specific angular momentum relation (SHSAMR) of galaxies at $z = 0$ by combining i) the standard Λ CDM tidal torque theory ii) the observed relation between stellar mass and specific angular momentum (Fall relation) and iii) various determinations of the stellar-to-halo mass relation (SHMR). We find that the ratio $f_j = j_*/j_h$ of the specific angular momentum of stars to that of the dark matter i) varies with mass as a double power-law, ii) it always has a peak in the mass range explored and iii) it is 3 – 5 times larger for spirals than for ellipticals. The results have some dependence on the adopted SHMR and we provide fitting formulae in each case. For any choice of the SHMR, the peak of f_j occurs at the same mass where the stellar-to-halo mass ratio $f_* = M_*/M_h$ has a maximum. This is mostly driven by the straightness and tightness of the Fall relation, which requires f_j and f_* to be correlated with each other roughly as $f_j \propto f_*^{2/3}$, as expected if the outer and more angular momentum rich parts of a halo failed to accrete onto the central galaxy and form stars (biased collapse). We also confirm that the difference in the angular momentum of spirals and ellipticals at a given mass is too large to be ascribed only to different spins of the parent dark-matter haloes (spin bias).

Key words: galaxies: fundamental parameters - galaxies: formation - galaxies: haloes - galaxies: spiral - galaxies: elliptical and lenticular, cD

1 INTRODUCTION

Mass and angular momentum are amongst the most important quantities underlying a physically motivated classification of galaxies. Inspired by this belief, Fall (1983) first looked at how galaxies were distributed in the plane $j_* - M_*$ of specific angular momentum and stellar mass. This pioneering work (based on data from Rubin et al. 1980; Davies et al. 1983) led to the discovery of an important scaling relation, which we can now call the *Fall relation(s)*: i) for a given morphological type, stellar mass and specific angular momentum of galaxies are related by a power-law, ii) spirals and ellipticals follow parallel sequences, with identical slopes but different normalizations, with ellipticals having approximately five times less specific angular momentum than spirals for a given stellar mass.

These findings were more recently confirmed by Romanowsky & Fall (2012, hereafter RF12), who compiled

measurements for a sample of ~ 100 nearby galaxies of all Hubble types for over three orders of magnitude in stellar mass, by Obreschkow & Glazebrook (2014), who measured angular momenta of stars, cold atomic and molecular gas in 16 nearby spirals and by Cortese et al. (2016), who extended the sample to ~ 500 nearby galaxies and studied both the stellar and warm gas specific angular momentum (though their measurements reached only one or two effective radii). Perhaps even more noteworthy is that the specific angular momentum-mass relation was recently measured also for star-forming disc galaxies at high redshift ($z \sim 1 - 2$) and it was found to be a power-law of similar slope and normalization as at $z = 0$ with the residuals correlating to galaxy morphology, as observed for nearby galaxies (Burkert et al. 2016; Harrison et al. 2017). Remarkably, the simple nature of the Fall relation (a power-law over several decades, with little scatter) is virtually identical to a theoretical relation which is expected to hold for the dark matter haloes from Tidal Torque Theory (TTT, see e.g. Peebles 1969; Efstathiou & Jones 1979).

* E-mail: posti@astro.rug.nl

The simple correspondence, in the specific angular momentum-mass diagram, between stars and dark matter could be interpreted as a major theoretical success, if one assumed that both the mass and the angular momentum of a galaxy are directly proportional to those of their haloes (with some dependence on morphology, but none on the mass). Indeed, some of the earliest theoretical models of galaxy formation (e.g. Fall & Efstathiou 1980; Dalcanton, Spergel, & Summers 1997; Mo, Mao, & White 1998) were based on these assumptions and turned out to be relatively successful in reproducing the observed structural properties and scaling relations of disc and spheroidal galaxies (for more recent similar models see e.g. Somerville et al. 2008; Dutton & van den Bosch 2012; Kravtsov 2013).

We now know, however, that at least one of the two assumptions above, i.e. that the stellar mass-to-halo mass ratio is constant with mass, is not correct. The stellar-to-halo mass relation (SHMR) is indeed rather complex and far from being linear as it emerged from several recent works, despite the different techniques used to estimate dark-matter halo masses. Consistent results were found in studies that made use of either the so-called abundance matching ansatz (see e.g. Vale & Ostriker 2004; Moster, Naab, & White 2013; Behroozi, Wechsler, & Conroy 2013), sometimes combined with direct estimates via weak lensing and stellar or satellite kinematics (see e.g. Leauthaud et al. 2012; van Uitert et al. 2016), or the spatial clustering of galaxies (see e.g. Yang, Mo, & van den Bosch 2003; Tinker et al. 2017) or the segregation by colour of galaxy populations (see e.g. Dutton et al. 2010; Rodríguez-Puebla et al. 2015). In the light of these findings, the simplicity of the observed Fall relation ceases to be a confirmation of expectations and rather starts to be a *theoretical challenge*. In particular, the following question naturally arises: what fraction of the specific angular momentum of haloes their galaxies need to have to be consistent simultaneously with the Fall relation and the SHMR? Addressing this question is the main aim of this paper.

From the observational point of view, only very few studies have tried to investigate somewhat similar questions: for instance, Kauffmann et al. (2015) have measured the specific angular momenta of ~ 200 massive gas rich galaxies from rotation curves, they have computed the fraction of stellar-to-halo specific angular momentum and found it to strongly correlate with galaxy mass. From the theoretical point of view, some models were already built upon the realisation that if the SHMR is not constant with mass, then galaxies should have a non-constant fraction of the specific angular momentum of their haloes (e.g. Navarro & Steinmetz 2000). More recently, also other authors have investigated similar questions to ours by means of semi-analytical models (e.g. Dutton & van den Bosch 2012; Stevens, Croton, & Mutch 2016), as well as of cosmological simulations (Genel et al. 2015; Pedrosa & Tissera 2015; Teklu et al. 2015; Zavala et al. 2016; Sokolowska et al. 2017). Despite going deep in physically-motivated prescriptions, all these studies either did not really try or fell short of reproducing the straightness and the small scatter of the Fall relation across its entire mass range and many did not really compare the predictions of their models on the specific angular momentum-mass diagram and on the SHMR at the same time, hence leaving unanswered questions on the galaxy-halo connection.

In the present contribution, we adopt a complementary

approach. Without assuming a specific scenario, we try to reconstruct the stellar-to-halo specific angular momentum relation (SHSAMR), as a function of mass and morphological type, by requiring the empirical Fall relation to be reproduced. We stress the inherent uncertainties of the process by systematically investigating the dependence of the results on the adopted SHMR. Then, we try to address some interesting related questions, such as i) whether the origin of the specific angular momentum-mass relation can be interpreted in terms of galaxies forming stars from the innermost and more angular momentum-poor part of the halo and ii) whether the different angular momenta between spirals and ellipticals can be ascribed to differences in the spin parameters of the host dark matter haloes.

The paper is organised as follows. In Section 2, we briefly review some observational and theoretical background concerning the angular momentum of the stellar and dark components of galaxies. In Section 3, we derive our SHSAMR for spirals and ellipticals, adopting different existing SHMR from the literature. In Section 4, we investigate the origin of the Fall relation with two physical models (biased collapse and spin bias). We summarize and conclude in Section 5.

Throughout the paper we use the standard Λ Cold Dark Matter (Λ CDM) model with the cosmological parameters estimated by the Planck Collaboration et al. (2016): $(\Omega_m, \Omega_\Lambda) = (0.31, 0.69)$ are the matter and dark energy density and $H_0 = 67.7 \text{ km s}^{-1} \text{ Mpc}^{-1}$ is the Hubble constant.

2 THE ANGULAR MOMENTUM OF GALAXIES AND THEIR HALOES

Here we introduce the framework with the equations relevant to our work. We begin by re-deriving the specific angular momentum of dark matter haloes in a standard Λ CDM Universe and then we relate this to galaxies by introducing the key parameters of our models.

2.1 The specific angular momentum of dark matter haloes

The mass distribution of a spherically symmetric dark matter halo whose density distribution is described by a Navarro, Frenk, & White (1996, hereafter NFW) profile, is characterized by two parameters: the mass within the virial radius M_h and the concentration c .

At $z = 0$, the virial radius of a halo of mass M_h is

$$r_{\text{vir}} = \left(\frac{2GM_h}{\Delta_c H_0^2} \right)^{1/3} \quad (1)$$

where $\Delta_c = 102.5$ is the virial overdensity w.r.t. to the critical density of the Universe (Bryan & Norman 1998).

The mass-concentration relation has been widely studied in the literature, especially by means of cosmological simulations (e.g. Navarro, Frenk, & White 1997) which have shown that the concentration has a weak dependence on halo mass. In the following we adopt the relation found by Dutton & Macciò (2014)

$$\log c = 0.537 - 0.097 \log[M_h / (10^{12} M_\odot / h)] \quad (2)$$

with an intrinsic scatter of about 0.11 dex.

Dark matter haloes acquire rotation from tidal torques exerted by the surrounding matter (see e.g. Hoyle 1949) and this is usually quantified with the so-called spin parameter

$$\lambda \equiv \frac{J|E|^{1/2}}{GM^{5/2}}, \quad (3)$$

where G is the gravitational constant and J , M and E are respectively the angular momentum, mass and energy of the system (see Peebles 1969). Cosmological simulations have shown that λ is log-normally distributed and independent on halo mass (e.g. Efstathiou & Jones 1979; Barnes & Efstathiou 1987; Porciani, Dekel, & Hoffman 2002). Here we adopt the results of Macciò et al. (2007), who found log-normal distributions with expectation value $\lambda \simeq 0.035$ and scatter of about 0.25 dex.

By inverting the definition of λ (equation 3), the specific angular momentum j_h of a dark matter halo can be conveniently expressed as

$$j_h \equiv \frac{J_h}{M_h} = \sqrt{\frac{2}{F_E(c)}} \lambda V_{\text{vir}} r_{\text{vir}}, \quad (4)$$

where

$$V_{\text{vir}} \equiv \sqrt{\frac{GM_h}{r_{\text{vir}}}} \quad (5)$$

is the halo circular velocity at the virial radius and

$$F_E \equiv -\frac{2E}{M_h V_{\text{vir}}^2}. \quad (6)$$

is a dimensionless factor that depends on the structure of the halo. Following Mo, Mao, & White (1998, their equation 23), we write F_E as a function of the concentration c :

$$F_E(c) = \frac{c}{2} \frac{[1 - 1/(1+c)^2 - 2 \ln(1+c)/(1+c)]}{[c/(1+c) - \ln(1+c)]^2}. \quad (7)$$

Combining equations (1), (4) and (5) we find that at $z = 0$ the specific angular momentum j_h of a halo of mass M_h is

$$\begin{aligned} j_h &= (\Delta_c H_0^2)^{-1/6} \frac{\lambda}{\sqrt{F_E(c)}} (2GM_h)^{2/3} \\ &= \frac{1.67 \times 10^3}{\sqrt{F_E(c)}} \left(\frac{\lambda}{0.035} \right) \left(\frac{M_h}{10^{12} M_\odot} \right)^{2/3} \text{ kpc km s}^{-1}, \end{aligned} \quad (8)$$

which is not very different from $j_h \propto M_h^{2/3}$, since the dependence of $\sqrt{F_E(c)}$ on halo mass is very weak¹ compared to the power-law $M_h^{2/3}$.

This is similar to the relation adopted by RF12, except for the fact that we use updated cosmological parameters and we take the dependence on the concentration into account.

¹ $F_E(c)$ varies about 20% in the mass range $10 \leq \log M_h/M_\odot \leq 14$.

2.2 The specific angular momentum of the stars

From equation (8), the average specific angular momentum of the stars in a galaxy can be written as

$$j_\star = \frac{77.4}{\sqrt{F_E(c)}} \left(\frac{\lambda}{0.035} \right) f_j f_\star^{-2/3} \left(\frac{M_\star}{10^{10} M_\star} \right)^{2/3} \text{ kpc km s}^{-1}, \quad (9)$$

where

$$f_\star \equiv \frac{M_\star}{M_h} \quad (10)$$

is the ratio of stellar mass to halo mass, while

$$f_j \equiv \frac{j_\star}{j_h} \quad (11)$$

is the ratio of the average specific angular momentum of the stars in the galaxy to that of the dark matter halo².

The ratio of stellar mass to halo mass f_\star is sometimes loosely referred to as *star formation efficiency*, although it encapsulates a variety of very different processes, including e.g. the actual efficiency of the conversion of gas into stars, the fraction of baryons which ever collapses to the centre of the halo (e.g. Kassin et al. 2012), the cumulative effect of feedback from star formation and accretion on the central black hole (e.g. Veilleux, Cecil, & Bland-Hawthorn 2005; Harrison 2017) and, finally, the effect of galactic fountains (which can engage a significant portion of gas in circulating in the circumgalactic medium at various distances from the star forming body of the galaxy, e.g. Fraternali & Binney 2008). Notice also that, by construction, f_\star is bound to be equal or smaller than the *cosmic baryon fraction* $f_b \equiv \Omega_b/\Omega_m = 0.157$ (Planck Collaboration et al. 2016).

Similarly, we will somewhat loosely refer to f_j in equation (11) as the *retained fraction of angular momentum*. This parameter depends on many phenomena, such as the angular momentum losses due to, e.g., dynamical friction of baryonic massive clumps or induced by galaxy mergers (see e.g. Aarseth & Fall 1980; Barnes 1992; Hernquist & Mihos 1995), but also on the possibility that galaxies form from the inner and less angular momentum rich portion of haloes (*biased collapse*, e.g. van den Bosch 1998, RF12), partially counteracted by the opposite effect, namely the selective removal of low angular momentum material as a consequence of galactic winds (e.g. Governato et al. 2007; Brook et al. 2011), and finally, to some extent, angular momentum redistributions due to galactic fountains (e.g. Brook et al. 2012; DeFelippis et al. 2017). Both estimates from recent observations (e.g. Cortese et al. 2016) and expectations from numerical simulations (e.g. Teklu et al. 2015) and semi-analytic models (e.g. Dutton & van den Bosch 2012) agree that this fraction should be of the order of $f_j \sim 0.1 - 0.5$ for all galaxies, even if in principle such fraction can be also larger than one.

As discussed in Section 1, observational determinations of the $j_\star - M_\star$ relation find a power-law dependence $j_\star \propto M_\star^\alpha$ with index α close to $2/3$ for each morphological type

² Equation (9) is also similar to the relation adopted by RF12, but for the adopted cosmology, the dependence on concentration and the fact that they normalize the stellar fraction by the cosmic baryon fraction.

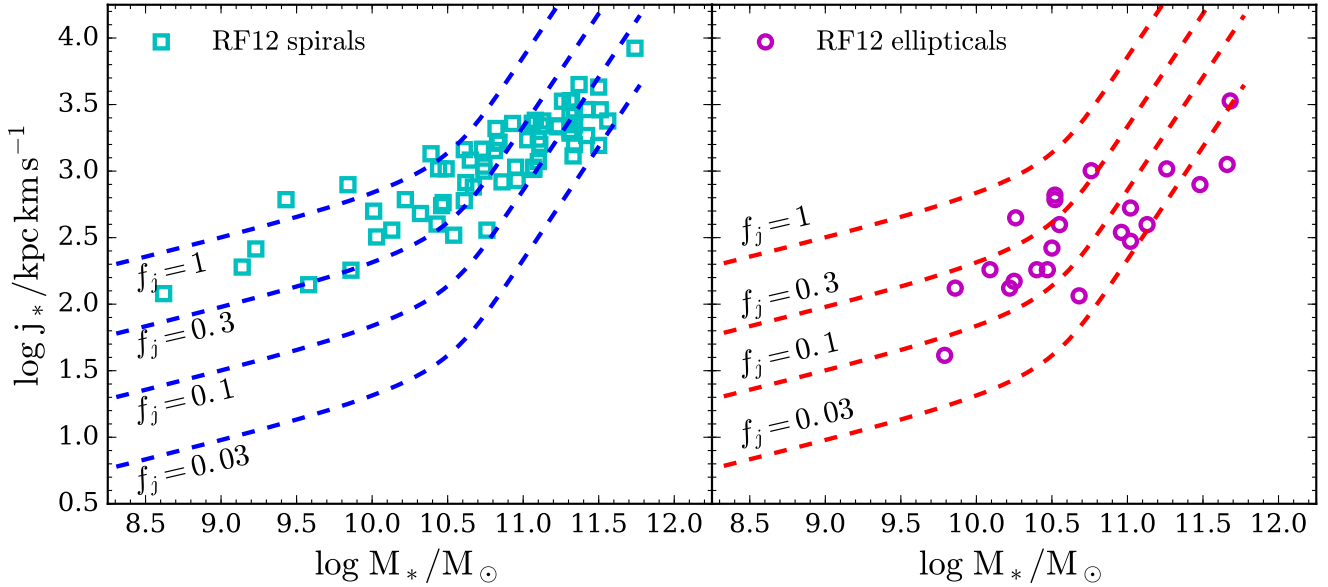


Figure 1. Specific angular momentum-mass diagram for a model with the SHMR of [Moster, Naab, & White \(2013\)](#) and a constant retained fraction f_j for late and early types in the left- and right-hand panel respectively (assuming $\lambda = 0.035$ for the dark matter haloes). Different curves are for different values of the constant $f_j = 1, 0.3, 0.1, 0.03$. The cyan squares and the magenta circles are data points for late and early types respectively from [RF12](#).

(the *Fall relation*). A comparison with equation (9) therefore suggests that the quantity

$$Q = \frac{\lambda}{F_E(c)} f_j f_*^{-2/3} \quad (12)$$

does not vary much with stellar or halo mass, at least for a fixed morphological type. Amongst the ways to have Q constant there is the possibility that both f_* and f_j are constant (e.g. [Mo, Mao, & White 1998](#)) or that f_* and f_j are correlated (e.g., [Navarro & Steinmetz 2000](#)).

In contrast, any model with varying f_* and constant f_j as a function of galaxy mass *are not expected to be in agreement with the data*. This is illustrated in Figure 1, where we plot for spirals (left panel) and ellipticals (right panel) the predictions on the specific angular momentum-mass diagram of a model, given by equation (9), with variable f_* and constant f_j . For this example, we fixed the spin and concentration of the haloes to a typical value ($\lambda = 0.035$ and $c = 10$) and we use the widely adopted SHMR of [Moster, Naab, & White \(2013\)](#). Clearly, none of the curves shown provides a satisfactory description of the data. This indicates that f_j is not constant, but rather varies with both mass and morphological type, being close to 0.5 for low-mass spirals and about 0.03 for the most massive galaxies of any type. This is true, at least, if both the *Fall relation* and the SHMR of [Moster, Naab, & White \(2013\)](#) are correct.

In the next Section we investigate the dependence of f_j on galaxy mass and morphological type in detail and for different choices of the SHMR.

3 THE RETAINED FRACTION OF ANGULAR MOMENTUM AS A FUNCTION OF GALAXY MASS AND TYPE

3.1 Summary of the model

We now derive the SHSAMR as a function of galaxy mass and morphological type by imposing that both the *Fall relation* and a given SHMR are satisfied. We proceed as follows:

- (i) we draw a sample of 10^5 galaxies from a uniform distribution³ in $\log M_*$ in the range $8.5 \leq \log(M_*/M_\odot) \leq 12$;
- (ii) to each galaxy we assign a dark matter halo whose mass is drawn from a normal distribution in $\log M_h$ with mean and standard deviation given by the adopted SHMR (see Section 3.2);
- (iii) we draw a spin parameter from a normal distribution in $\log \lambda$ with mean $\lambda = 0.035$ and standard deviation of 0.25 (see Section 2.1);
- (iv) we draw a concentration c from a normal distribution in $\log c$ whose mean and standard deviation are given by the $c(M_h)$ as in equation (2);
- (v) we compute j_h using equation (8);
- (vi) we draw the stellar specific angular momentum j_* from a normal distribution in $\log j_*$ with mean and standard deviation as estimated by [RF12](#). In particular we use the two

³ Since we are interested in the behaviour of some scaling relations and not in galaxy/haloes number densities, we do not need to adopt a more realistic galaxy mass function. We work with a uniform mass function for clarity of the presentation of the results.

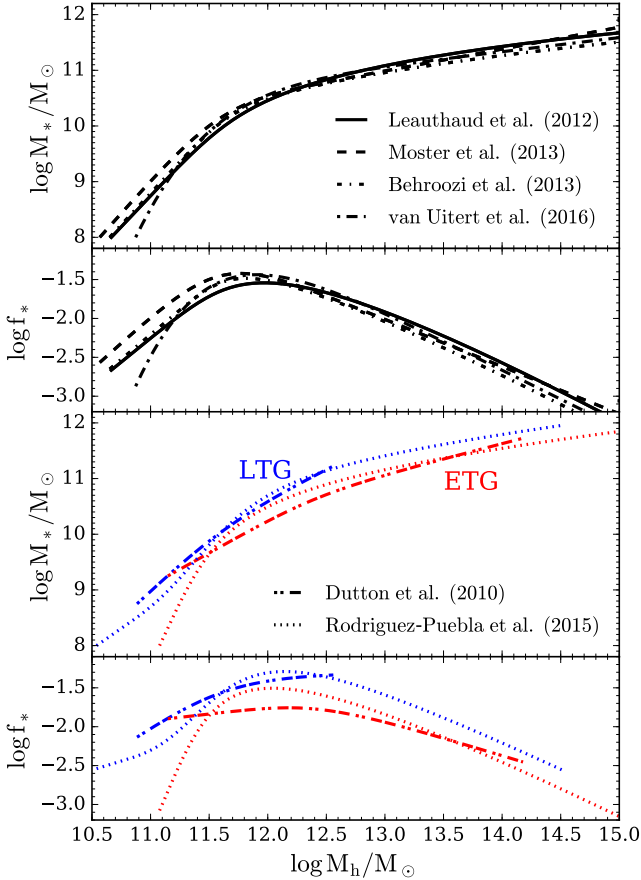


Figure 2. The mean SHMR and the corresponding $f_* = f_*(M_h)$ for the two parametrisations derived for different galaxy types (bottom panels, blue for late types and red for early types) and the other four adopted in this work (top panels).

following estimates of the Fall relation:

$$\log j_* = 3.18 + 0.52 [\log(M_*/M_\odot) - 11], \quad \sigma_{\log j_*} = 0.19, \quad (13)$$

for late-type galaxies in the stellar mass range $8.62 \leq \log(M_*/M_\odot) \leq 11.74$ and

$$\log j_* = 2.73 + 0.60 [\log(M_*/M_\odot) - 11], \quad \sigma_{\log j_*} = 0.24, \quad (14)$$

for early-type galaxies in $9.79 \leq \log(M_*/M_\odot) \leq 11.94$, where $\sigma_{\log j_*}$ is the root mean square scatter. ;

(vii) we compute $f_j = j_*/j_h$.

Note that this procedure implicitly assumes that the scatters of all the adopted relations are uncorrelated. The implications of this assumption are discussed in Section 3.4.

For simplicity, in what follows we will use the terms late-type and early-type galaxy as synonyms for spiral and elliptical galaxy. This implies, for instance, that we are assuming that the population of spirals and ellipticals of RF12 traces the population of blue and red galaxies when we adopt colour-segregated SHMR (Dutton et al. 2010; Rodríguez-Puebla et al. 2015). Also, we do not explicitly treat intermediate galaxy types, e.g. S0s, for which the $j_* - M_*$ relation would be intermediate between equations (13) and (14), see RF12. However, in this work we are interested in the *main*

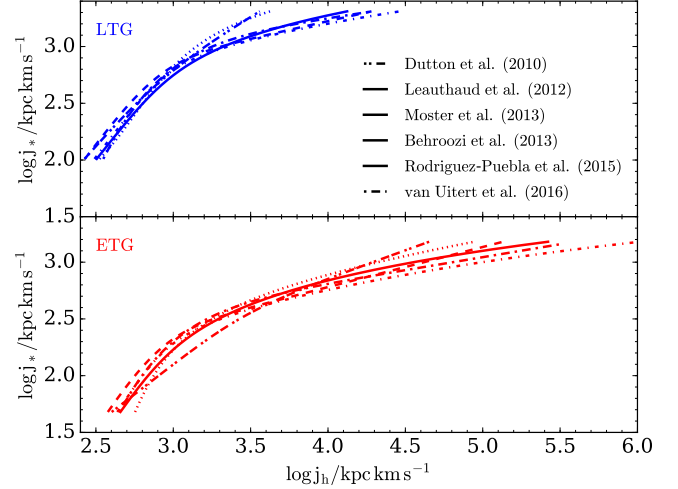


Figure 3. The mean SHSAMR for late- (top panel) and early-type galaxies (bottom panel) for six different SHMR. This relation is computed in the stellar mass ranges probed by the measurements of spirals and elliptical galaxies from RF12.

trends of the galaxy populations as a function of morphological type and mass and we expect this rather crude distinction to capture them.

3.2 The SHMR

We employ six different parametrisations of the SHMR amongst those available in the literature. We consider three types of SHMR and two examples per type.

The first two are derived by imposing that the cumulative mass function of haloes matches the observed cumulative galaxy stellar mass function, i.e. the so-called *abundance matching* technique (see e.g., Vale & Ostriker 2004). We adopt in particular the two very popular models by Behroozi, Wechsler, & Conroy (2013) and Moster, Naab, & White (2013), which are constrained using the largest compilation of galaxy stellar masses available (including galaxies of all types) at different redshifts. We show the (mean) SHMR and the corresponding f_* in Figure 2 (top panels). The scatter of these two relations is about ~ 0.15 dex

The second set of SHMR we consider is derived combining constraints from the abundance matching hypothesis together with empirical estimates of M_* and M_h for individual objects, e.g. from stellar, gas or satellite kinematics or from weak galaxy-galaxy lensing. This should, in principle, lead to a better estimation of the global SHMR. Note, however, that including individual objects in the fit may bias the results towards a given population of galaxies (e.g. galaxies with well-behaved gas discs if one uses gas kinematics or galaxies in crowded environments if one uses weak galaxy-galaxy lensing). In this work we consider the two parametrizations of Leauthaud et al. (2012) and van Uitert et al. (2016), which we plot in Figure 2 (top panels). The scatter of these two relations is about 0.19 dex and 0.15 dex respectively.

Finally, we use two SHMR that have been estimated separately for galaxies with red and blue colours (either with pure abundance matching or by combining different constraints) and in particular those of Dutton et al. (2010) and

Rodríguez-Puebla et al. (2015). The first attempt in this direction was that of Dutton et al. (2010). However, this study has a few limitations: i) the stellar mass range probed is small ($9.7 \lesssim \log(M_*/M_\odot) \lesssim 11.2$ for spirals), ii) measurements of both abundance matching models and stellar/halo masses for individual galaxies have improved since 2010 and iii) the best-fitting function itself is found by eye. All these reasons probably lead to a rather flat estimate of f_* for spirals galaxies if compared to those of many other works (see e.g. Figure 2). The more recent work by Rodríguez-Puebla et al. (2015) improved over these issues as i) they probe a much larger mass range $9 \lesssim \log(M_*/M_\odot) \lesssim 12$, ii) they use updated data and methods to match the stellar/halo mass functions and iii) they use an automatic routine to find the best-fitting parameters of their model. We will, however, still consider the SHMR by Dutton et al. (2010) in order to be able to compare our results with those of Dutton & van den Bosch (2012), who first inferred the $f_j - M_h$ for spiral galaxies. We show these two SHMR segregated by galaxy type in Figure 2 (bottom panels).

3.3 The SHSAMR and the distribution of f_j as a function of mass

Figure 3 shows the mean relation between the specific angular momentum of stars and dark matter (SHSAMR) that we obtain assuming six different parametrisations of the SHMR. This relation is computed separately for spiral and elliptical galaxies and in both cases it is found to be highly non-linear (in $\log j_h - \log j_*$), irrespectively of the SHMR adopted. Similarly to the relation between stellar mass and halo mass, galaxies on average follow a rather steep SHSAMR at low- j_h , which becomes shallower for large galaxies found at higher specific angular momenta.

We now study the full distributions of the retained fractions f_j as a function of halo mass M_h (Figure 4) and stellar mass M_* (Figure 5) for the six different SHMR. For each SHMR we plot the mean relation for late- and early-type galaxies together with a shaded area indicating its uncertainty given the current data, which results from the composition of the scatters in the observed $j_* - M_*$, the SHMR, the $c - M_h$ and the distribution of λ . We discuss this point in detail in Section 3.4.

At a fixed halo mass, the retained fraction of angular momentum is dependent on galaxy's morphology, with late-type galaxies having f_j systematically larger than that of early-type galaxies by roughly a factor 3–5, consistent with the findings of RF12. For a fixed morphological type, f_j generally has a maximum at the halo mass M_{peak} corresponding to the peak of f_* (at about $\log M_h/M_\odot \simeq 12$ for all the SHMR adopted here, see Figure 2). For all the six SHMR the mean f_j tends to mildly decrease at masses smaller than M_{peak} , by roughly a factor of ~ 2 at $\log(M_h/M_\odot) = 11$. At masses much larger than M_{peak} all models (but that with the SHMR by Dutton et al. 2010, which does not extend to that mass range) exhibit a sharp decrease of the mean f_j , by roughly a factor 3–5 at $\log(M_h/M_\odot) = 13.5$. Given the scatter that we estimate for these distributions (see Section 3.4 for details) the variation of f_j with halo mass is significant in all models, except those with the SHMR by Dutton et al. (2010) which are consistent with a constant $f_j \simeq 0.5$ for spirals and $f_j \simeq 0.1$ for ellipticals. However,

by comparing the top right panel of Figure 4 with the other panels it is clear that this result is mainly driven by the small mass range probed by that specific SHMR. From this we conclude that the finding of Dutton & van den Bosch (2012) that f_j is approximately constant with galaxy mass is mainly due to their choice of the SHMR. Finally, we notice that in the mass range observationally probed by the Fall relation of RF12 (darker shaded areas and curves in Figures 4–5) also the distribution of f_j for spiral galaxies with the SHMR of Rodríguez-Puebla et al. (2015) appears to be marginally consistent with a constant $f_j \simeq 0.4$ even if the mean f_j sharply decreases at large masses. This is because the scatter we have conservatively estimated is rather large (see Section 3.4). Similar trends are present in the distribution of f_j as a function of stellar mass M_* , thus similar conclusions can be drawn from Figure 5.

One of the main results of our work is that the detailed shape of the distribution of f_j as a function of halo mass significantly depends on the SHMR. As discussed in Section 2.2, if the Fall relation is a power-law for each morphological type, then f_j must decrease for masses larger (and smaller) than M_{peak} by an amount that balances the decrease of $f_*^{2/3}$. In particular, $j_* \propto M_*^\alpha$ and a mass-independent spin parameter λ for the dark matter yield

$$f_j \propto \frac{M_*^\alpha}{M_h^{2/3}} = f_*^{2/3} M_*^{\alpha-2/3}. \quad (15)$$

In particular, if f_* varies as a power-law $f_* \propto M_*^\beta$ in a given stellar mass range, then in the same range f_j also behaves as a power-law

$$f_j \propto M_*^{\alpha+\frac{2}{3}(\beta-1)}, \quad (16)$$

or, equivalently, if f_* varies as $f_* \propto M_h^\gamma$ in a given halo mass range, then f_j goes as

$$f_j \propto M_h^{\alpha(\gamma+1)-\frac{2}{3}}. \quad (17)$$

In the stellar mass range probed by RF12 the Fall relations for spirals and ellipticals have $\alpha = 0.52$ and $\alpha = 0.60$, respectively. For spiral galaxies, for instance, this implies that for a Dutton et al. (2010) SHMR the retained fraction f_j roughly behaves as $f_j \propto M_h^{0.37}$ and $f_j \propto M_h^{-0.15}$ at low- and high-masses respectively; while for a Moster, Naab, & White (2013) SHMR equations (16)-(17) imply the behaviours $f_j \propto M_h^{0.57}$ and $f_j \propto M_h^{-0.46}$ at low- and high-masses respectively.

Our results are a consequence of the fact that the empirical Fall relation is well represented by a single power-law of index close to 2/3. All the observations available at the moment are consistent with a power-law $j_* - M_*$ relation, whose normalization (and maybe logarithmic slope) vary with galaxy morphology. However, it is not definitively clear whether an upward bend of such relation for very massive ($\log M_*/M_\odot > 11.5$) discs can be completely ruled out (see e.g. Fall & Romanowsky 2013) and the determination of j_* for the most massive nearby disc galaxies known would be extremely helpful in shedding some light on this issue. At stellar masses smaller than $\sim 10^9 M_\odot$ observational constraints on both the Fall relation and the SHMR are either very uncertain or missing, hence our conclusions can not reliably extend much further down this mass. However, if

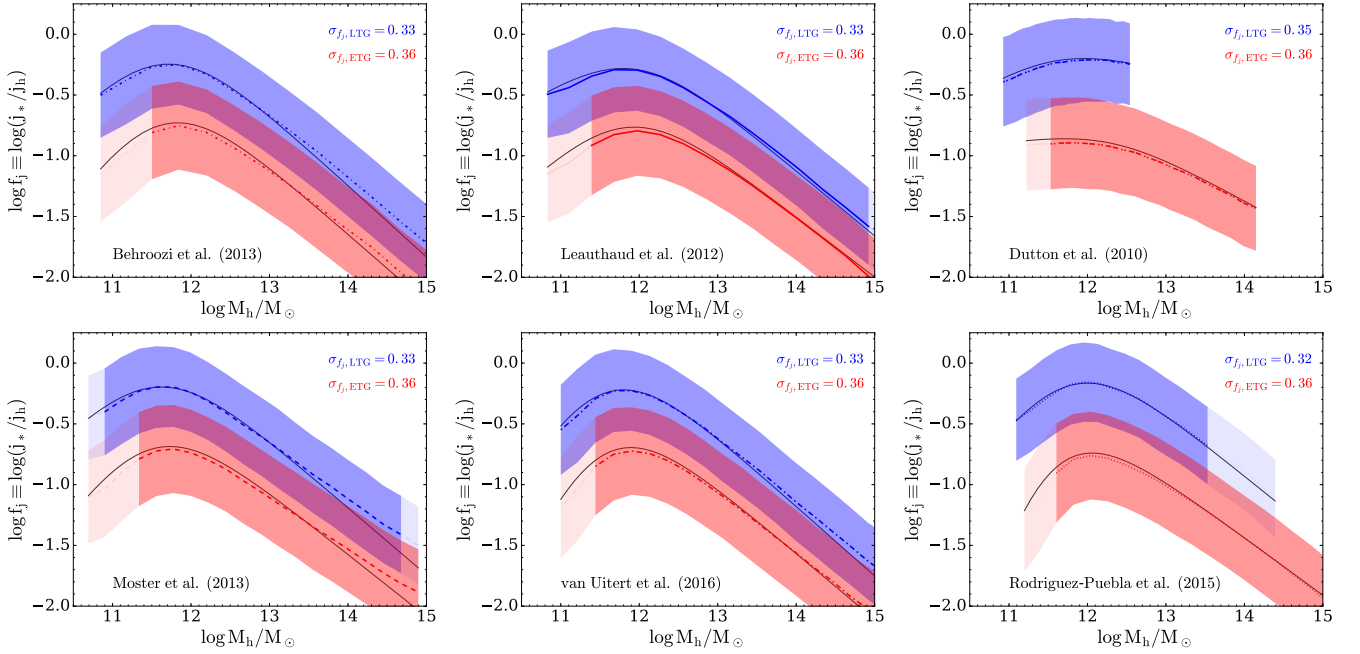


Figure 4. Ratio of stellar to halo angular momentum as a function of halo mass for six models with different SHMR. In all the six panels the blue and red curves (shaded regions) are the mean (1σ interval) for the late-type and early-type galaxies respectively. The models are plotted in the fiducial galaxy mass range for the given SHMR. Darker shaded areas denote the mass range probed by RF12. Lighter areas assume an extrapolation of the best fit power-law of RF12 beyond that range. The right panels are for models with different SHMR for the two galaxy types, while the left and central panels are for those which have the same SHMR for both types. In each panel we also plot, with thin black solid curves, the best-fit double power-law $f_j(M_h)$ parametrized as in equation (18). The values of the best-fit parameters are given in Table 1. In the top-right of each panel we also write the average 1σ scatter in $\log f_j$ at a fixed halo mass for the two galaxy types, also visible as shaded areas.

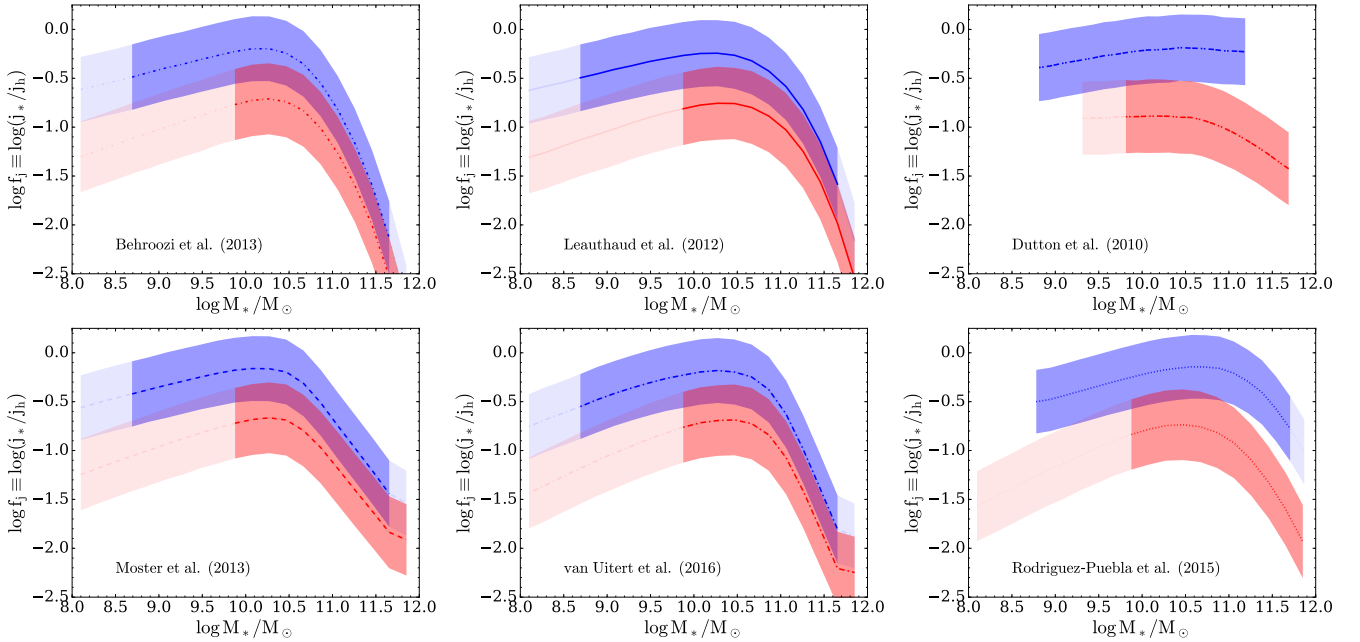


Figure 5. Same as Figure 4, but as a function of the stellar mass.

Table 1. Best parameters and corresponding $1 - \sigma$ uncertainties of a double power-law model of the type $f_j = f_{j,0} (M_h/M_0)^a (1 + M_h/M_0)^{b-a}$ (equation 18) fitted to the $f_j - M_h$ relation of the various models in Figure 4.

Model	$f_{j,0}$	$\log M_0/M_\odot$	a	b
<i>Late type galaxies</i>				
Behroozi, Wechsler, & Conroy (2013)	$1.9^{+0.05}_{-0.06}$	$11.65^{+0.06}_{-0.06}$	$0.67^{+0.05}_{-0.07}$	$-0.57^{+0.04}_{-0.04}$
Moster, Naab, & White (2013)	$1.96^{+0.05}_{-0.05}$	$11.54^{+0.05}_{-0.05}$	$0.6^{+0.08}_{-0.05}$	$-0.54^{+0.05}_{-0.05}$
Leauthaud et al. (2012)	$1.35^{+0.04}_{-0.04}$	$11.85^{+0.06}_{-0.06}$	$0.44^{+0.03}_{-0.03}$	$-0.52^{+0.03}_{-0.03}$
van Uitert et al. (2016)	$2.42^{+0.1}_{-0.08}$	$11.53^{+0.06}_{-0.06}$	$1.1^{+0.1}_{-0.1}$	$-0.59^{+0.03}_{-0.03}$
Dutton et al. (2010)	$1.17^{+0.07}_{-0.06}$	$11.8^{+0.2}_{-0.2}$	$0.34^{+0.04}_{-0.05}$	$-0.19^{+0.05}_{-0.08}$
Rodríguez-Puebla et al. (2015)	$2.31^{+0.06}_{-0.06}$	$11.77^{+0.05}_{-0.05}$	$0.87^{+0.05}_{-0.06}$	$-0.52^{+0.02}_{-0.02}$
<i>Early type galaxies</i>				
Behroozi, Wechsler, & Conroy (2013)	$0.68^{+0.08}_{-0.06}$	$11.6^{+0.1}_{-0.2}$	$0.9^{+0.2}_{-0.2}$	$-0.6^{+0.1}_{-0.1}$
Moster, Naab, & White (2013)	$0.7^{+0.05}_{-0.06}$	$11.5^{+0.1}_{-0.1}$	$0.8^{+0.1}_{-0.2}$	$-0.52^{+0.05}_{-0.05}$
Leauthaud et al. (2012)	$0.5^{+0.04}_{-0.04}$	$11.8^{+0.2}_{-0.2}$	$0.6^{+0.1}_{-0.1}$	$-0.5^{+0.1}_{-0.1}$
van Uitert et al. (2016)	$0.92^{+0.1}_{-0.08}$	$11.5^{+0.2}_{-0.1}$	$1.5^{+0.4}_{-0.3}$	$-0.57^{+0.06}_{-0.07}$
Dutton et al. (2010)	$0.24^{+0.04}_{-0.03}$	$12.3^{+0.4}_{-0.5}$	$0.09^{+0.1}_{-0.07}$	$-0.36^{+0.08}_{-0.1}$
Rodríguez-Puebla et al. (2015)	$0.9^{+0.1}_{-0.1}$	$11.3^{+0.1}_{-0.2}$	$2.6^{+0.6}_{-0.8}$	$-0.47^{+0.05}_{-0.05}$

we were to extrapolate the behaviour of both the Fall relation and the SHMR to the dwarf galaxies regime, we would find that f_j decreases with decreasing galaxy mass. At the moment there are only some indications that the Fall relation may be extended through the dwarf regime (Chowdhury & Chengalur 2017) and some studies which estimate the SHMR for dwarfs and compare it to that of more massive galaxies (e.g. Miller et al. 2014), so we are not able to draw any significant conclusion here. However, we notice that our expectation of a decreasing retained fraction f_j with decreasing stellar mass below $10^9 M_\odot$ is in agreement with the recent hydrodynamical simulations of El-Badry et al. (2017), whose model galaxies closely follow the SHMR of Moster, Naab, & White (2013), at least for $M_* > 10^{8.5} M_\odot$.

3.3.1 A simple description of the $f_j - M_h$ relation

We find that a reasonable description of the mean f_j as a function of M_h is provided by the following double power-law model

$$f_j = f_{j,0} \left(\frac{M_h}{M_0} \right)^a \left(1 + \frac{M_h}{M_0} \right)^{b-a} \quad (18)$$

where $f_{j,0}$, M_0 , a and b are constants representing respectively a normalization, a mass scale and the low- and high-mass slopes. In Table 1 we report the best-fit values of the above parameters to the twelve distributions of f_j as a function of halo mass, in the range of stellar masses probed by the RF12 Fall relations, presented in Figure 4 (found by minimising a χ^2 likelihood) together with their 1σ uncertainties (computed by sampling the posterior distribution using a Monte Carlo Markov Chain method, assuming uninformative priors). The values of the best-fitting low-mass and high-mass slopes a and b can be compared to the scaling given in equation (17) for a power-law Fall relation and in the regimes where the SHMR is approximated by a power-law.

3.4 Scatter of the SHSAMR

The large shaded areas in Figure 4 derive from a combination of the intrinsic and observational scatters in the $j_* - M_*$ plane and SHMR, as well as from the intrinsic scatter of the theoretical $c(M_h)$ relation and λ distribution. Each of these scatters sum up in quadrature to yield the final width

$$\tilde{\sigma}_{f_j} = \sqrt{\sigma_{j_*,\text{obs.}}^2 + \sigma_{\text{SHMR}}^2 + \sigma_{c-M_h}^2 + \sigma_\lambda^2} \sim 0.32 - 0.36 \text{ dex}, \quad (19)$$

While encompassing the current uncertainties, this should not be considered as an estimate of the intrinsic scatter of the SHSAMR σ_{f_j} , unless one makes the assumption that all the terms in equation (19) are uncorrelated, which is not very realistic, considering that at least the observed scatter $\sigma_{j_*,\text{obs.}}$ will most likely depend on σ_{SHMR} , σ_{c-M_h} and σ_λ . Thus, the width of the shaded areas should be regarded as a very conservative *upper limit* on the intrinsic scatter of the $f_j - M_h$ relation.

The observed scatter $\sigma_{j_*,\text{obs.}}$ of the $j_* - M_*$ relation is found to be much smaller than the sum in quadrature of σ_{SHMR} , σ_{c-M_h} and σ_λ (see Table 2). This suggests that the scatters of these quantities are likely to be correlated in such a way that when combined as in equation (9) they yield a scatter of ~ 0.19 dex for the j_* of spirals and ~ 0.24 dex for that of ellipticals. Note that these conclusions are mostly driven by the scatter in λ (see Table 2), which is theoretically well established.

The considerations above are critical also to interpret the results on the mass-dependence of the retained fraction. For instance, the f_j distribution of spirals in the case of the SHMR of Rodríguez-Puebla et al. (2015) is consistent with a constant only if the intrinsic scatter of the SHSAMR is as large as the displayed shaded area, which we argued above to be rather unlikely.

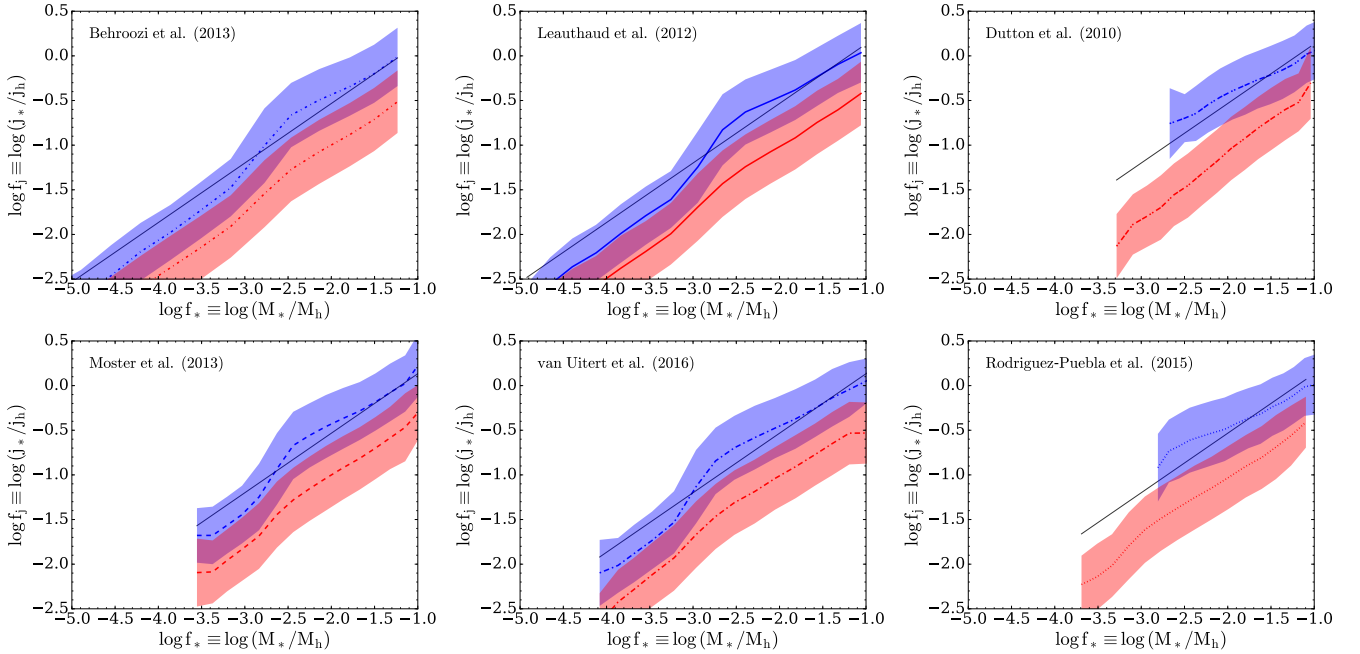


Figure 6. Retained fraction of angular momentum as a function of the stellar fraction, or star formation efficiency, for the same models as in Figure 4. We also show the proportionality $f_j \propto f_*^{2/3}$ as a grey thin solid line.

Table 2. Scatter budget (in dex) as in equations (19)-(??). The scatter of the SHMR are for the model of Rodríguez-Puebla et al. (2015) and observational estimates are from RF12 (see equations 13 and 14 above).

Galaxies	σ_λ	σ_{c-M_h}	σ_{SHMR}	$\sigma_{j_*, \text{obs.}}$
Late types	0.25	0.11	0.11	0.19
Early types	0.25	0.11	0.14	0.24

3.5 The distribution of f_j as a function of f_*

In Figure 6 we show the retained fraction of angular momentum f_j as a function of the stellar fraction, or star formation efficiency, f_* . These two quantities are clearly correlated such that galaxies with smaller stellar fraction also have smaller retained fraction of angular momentum. The correlation roughly follows $f_j \propto f_*^{2/3}$, so that the quantity Q defined in equation (12) is about constant with galaxy mass. The deviations of the observed Fall relation from $j_* \propto M_*^{2/3}$ can be interpreted as a consequence of the deviations of the $f_j - f_*$ relation from $f_j \propto f_*^{2/3}$ (see equation 15).

Note that similar conclusions to ours can be reached by modelling galaxies that are on the mass-rotational velocity relation, i.e. the Tully & Fisher (1977) relation, within a Λ CDM framework. Combining a $M_* \propto V_{\text{rot}}^3$ relation with the scalings for dark matter haloes summarized in Section 2.1 one finds $f_j \propto f_v^2$ where $f_v \equiv V_{\text{rot}}/V_{\text{max}}$, which also immediately yields $f_j \propto f_*^{2/3}$ (see Navarro & Steinmetz 2000). Currently this type of models are able to reasonably represent the observed Tully-Fisher, mass-size and SHMR simultaneously (see Ferrero et al. 2017). However, even if the

Tully-Fisher relation is much tighter and much better known w.r.t. the Fall relation, unlike the angular momentum retention fraction f_j which is directly related to the main phenomena driving galaxy evolution (e.g. the accretion history and feedback), the parameter f_v has no clear physical meaning and its link with galaxy evolution is much more obscure.

The $f_j - f_*$ relation indicates that *galaxies which are globally efficient at forming stars are also efficient at “retaining” angular momentum*. Hence the formation history of a galaxy which has very efficiently turned its available gas into stars is such that its spin is comparable to that of the dark halo (and viceversa), as cosmological hydrodynamical simulations also suggest. Recent studies have found that such galaxy/halo mass- and spin-connection is regulated either by the effect of stellar feedback, which preferentially removes the low- j material (see Pedrosa & Tissera 2015; DeFelippis et al. 2017), together with the halo assembly history, since mergers tend to lower the angular momentum of stars (see Sokolowska et al. 2017), and/or by the accretion history of gas onto the galaxy, which proceeds from the low- j material first and then continues to the high- j one for systems which are still efficient at forming stars at later times (see El-Badry et al. 2017). In Section 4 we expand the discussion of this latter kind of models, which we call *biased collapse* models following RF12.

All these factors potentially play key roles in shaping galaxies as we see them today and they must be considered when attempting to explain the current morphology and structural properties of galaxies. Any galaxy formation model, which aims at explaining the formation and evolution of galaxies in terms of their history of accretion and star formation, has necessarily to deal with the fact that the global star formation efficiency is intimately linked to the global efficiency at angular momentum retention.

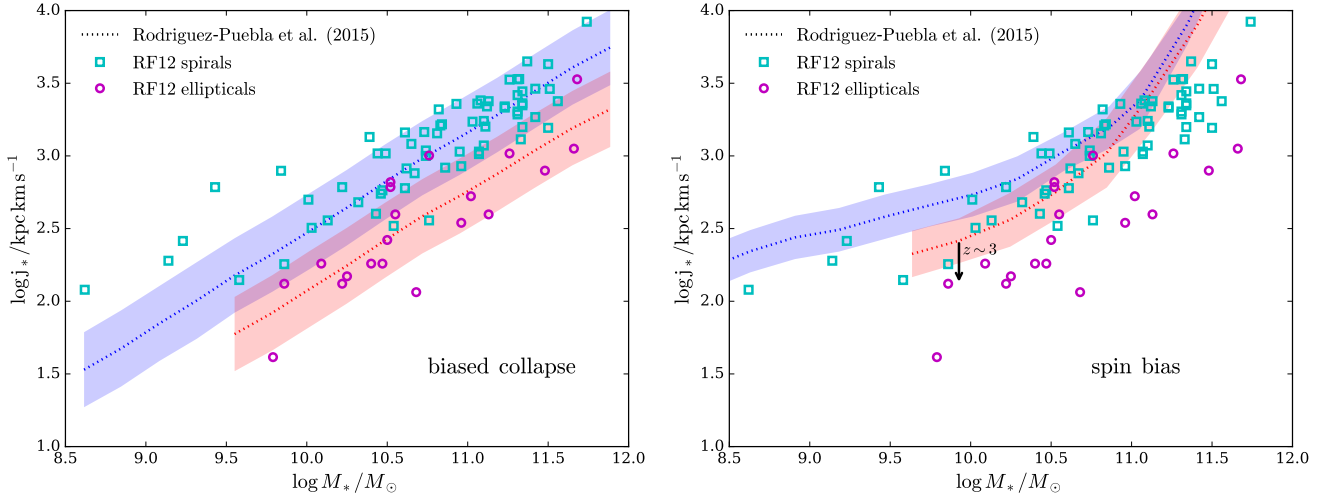


Figure 7. *Left-hand panel:* Fall relation for the biased collapse model in which $f_j \propto f_*^s$ (see Section 4.1). The blue and red shaded areas are the 1σ predictions of the models (the dotted curve is the mean), while the cyan squares and magenta circles are the late- and early-type galaxies observed by RF12. The models employ the SHMR of Rodríguez-Puebla et al. (2015) for each galaxy type. *Right-hand panel:* same as the left-hand panel, but for the spin-bias model in which the halo spin correlates with galaxy type (see Section 4.2). In this model we adopt a common $f_j = 0.5$ for spirals and ellipticals, while the black arrow shows the effect of assuming that all ellipticals were already quenched at $z = 3$.

4 PHYSICAL MODELS FOR THE ANGULAR MOMENTUM OF GALAXIES

In this Section we describe two simple physically-based models for the angular momentum content of galaxies and we compare their predictions on the specific angular momentum-mass diagram with observations from RF12. This approach is complementary to that adopted in Section 3 and may be useful to test the predictions of some specific scenarios. In particular, we first ask whether a power-law Fall relation naturally emerges in a *biased collapse scenario*, in which the global efficiency of star formation correlates with the efficiency at angular momentum retention (Section 4.1); then we ask whether the different normalization of the Fall relations for spirals and ellipticals can be ascribed to a *spin-bias* scenario and not to a variable f_j with galaxy mass (Section 4.2). For simplicity, here we use only the SHMR of Rodríguez-Puebla et al. (2015) and we are implicitly assuming that their blue and red galaxy populations trace the spirals and ellipticals of RF12.

4.1 Biased collapse models: a power-law $f_j - f_*$ relation

We first test a simple model in which f_j varies with galaxy mass. f_j and f_* are strongly correlated both in an empirical Λ CDM model based on the Fall relation (Section 3 and Figure 6) and in one based on the Tully-Fisher relation (see Navarro & Steinmetz 2000, and Section 3.5). The same happens also in a model in which the global star formation efficiency depends on the gas cooling efficiency: if the gas has a cumulative angular momentum distribution $j_{\text{gas}}(< r) \propto M_{\text{gas}}(< r)^s$ and it is accreted (and cools) onto the galaxy inside-out, then (see van den Bosch 1998; Dutton & van den Bosch 2012)

$$f_j = (f_*/f_b)^s, \quad (20)$$

where $f_b \equiv \Omega_b/\Omega_m$ is the cosmic baryon fraction. Hence f_* is expected to correlate with f_j if stars form preferentially from the gas at highest densities, i.e. closest to the centre where the gas cooling was more effective (e.g. Kassin et al. 2012, see also RF12, Section 6.3.2). We refer to this scenario as *biased collapse*.

In the model presented in this Section we interpret f_j as the *fraction of the halo's specific angular momentum present in the gas actually able to cool and form stars in the galaxy*. In practice, we are considering galaxies formed out of gas at angular momentum j between $0 \leq j \leq j_{\text{max}} < j_{\text{vir,DM}}$, where j_{max} is the maximum specific angular momentum of the material that collapsed to form the central galaxy. A correlation between f_j and f_* is expected also in the presence of feedback (as it is seen in cosmological simulations, e.g. Pedrosa & Tissera 2015), though it may alter the value of the exponent s in equation (20) due to angular momentum mixing (see below).

Motivated by these results we make the ansatz:

$$\log f_j = A + s \log f_*, \quad (21)$$

We repeat the steps (i) to (iv) as in Section 3.1, with the SHMR of Rodríguez-Puebla et al. (2015); then, we assign f_j to each galaxy as in equation (21), with variable A and s and no scatter; finally, we use equation (9) to compare with the observations of RF12.

We determine A and s by minimising a χ^2 likelihood and we also allow for the presence of outliers in the observed data. Then, we compute the posterior probabilities of the two parameters by assuming flat priors (using a Monte Carlo Markov Chain method). We obtain

$$A = 0.65 \pm 0.13, \quad s = 0.68 \pm 0.05, \quad (\text{spirals}) \quad (22)$$

$$A = 0.23 \pm 0.12, \quad s = 0.69 \pm 0.05. \quad (\text{ellipticals}) \quad (23)$$

Our model estimates a fraction of $f_{\text{out}} = 0.10 \pm 0.06$ of possible outliers in the Fall relation for spirals at $\log M_* \lesssim 10$,

while it is consistent with zero for ellipticals. The slope of the relation (21) is unsurprisingly in agreement with the value $2/3$ for both galaxy types: in fact, this is the only value of s that generates a power-law Fall relation (also with slope $2/3$). For reference, the case $f_j = 1$ would correspond to $s = 0$ in equation 21 (e.g. Mo, Mao, & White 1998, RF12) and we find it to be disfavoured by observations. On the other hand, our best fit value $s \simeq 0.7$ is significantly smaller than the value $s \simeq 1.3$ suggested by (Dutton & van den Bosch 2012), under the assumption that the baryons and the dark matter have exactly the same angular momentum distribution. Note that equation (20) is consistent with an angular momentum distribution of baryons $dM/dj \propto j^q$ with $s = 1/(1+q)$. The best fit $s = 0.68$ would imply $q = 0.47$, which is interestingly in between the values $q \simeq 0$ and $q \simeq 1$ expected for a dark matter halo and a pure disc, respectively (e.g. van den Bosch, Burkert & Swaters 2001). This may be an indication of mixing processes, possibly related to feedback, having redistributed the angular momentum of baryons, resulting in a shallower angular momentum distribution (e.g. Brook et al. 2012).

Remarkably, the value of the normalization for spirals is consistent with $A = -0.68 \times \log(f_b) = 0.55$, as expected from equation (20) with $s = 0.68$. For ellipticals, dynamical friction induced by mergers may have contributed to net losses of angular momentum resulting in an overall smaller normalisation.

We show in the left-hand panel of Figure 7 the predictions of this model compared with the galaxies observed by RF12. A remarkable agreement can be appreciated. Though, the scatter of the predicted relation is still too large compared to the observed scatter: the model predicts 0.26 dex w.r.t. the observed 0.19 dex and 0.24 dex for late and early types. This is because, as discussed in Section 3.4, we are overestimating the scatter of the Fall relation since we are assuming the scatters in the SHMR, λ distribution, $c(M_h)$ and $f_j - f_*$ relations to be uncorrelated. Moreover, even with this simplified assumption of no-intrinsic scatter in the $f_j - f_*$ relation we are still overpredicting the scatter in the $j_* - M_*$ relation.

4.2 Spin-bias models: low-rotating galaxies in low-spin haloes

Another hypothesis one could envisage is that the retention fraction f_j is actually constant with mass and galaxy type and, instead, the scatter of the halo spin distribution correlates with galaxy type and specific angular momentum. In this picture, at a fixed halo mass, haloes with larger spins host preferentially galaxies of later morphological types and with larger specific angular momenta (see e.g. RF12, Section 6.2). We refer to this scenario as *spin-bias*.

To test this hypothesis, we consider a model in which, for a given halo mass, the haloes with the largest λ are occupied by spirals and those with the smallest λ are occupied by ellipticals. In our simplified picture of galaxies of two morphological types well traced by their colours, we can define for each halo mass a critical value λ_{crit} which divides haloes populated by galaxies of the two types. This must be a function of mass $\lambda_{\text{crit}}(M_h)$ since haloes of different masses have different probabilities to contain galaxies of a given type (i.e. morphology depends on galaxy mass, e.g. Kelvin

et al. 2014). To find the function $\lambda_{\text{crit}} = \lambda_{\text{crit}}(M_h)$ we use an iterative procedure. Starting from a given SHMR and an observed distribution of late/early types fraction as a function of stellar mass $f_T = f_T(M_*)$, taken from Kelvin et al. (2014), we proceed as follows:

- (i) we generate a uniform population of $N_{\text{haloes}} = 10^5$ in $10 \leq \log M_h/M_\odot \leq 14$ and we divide it into 12 equally-spaced bins;
- (ii) starting from a flat guess for the function $\lambda_{\text{crit}}(M_h)$, in a given halo mass bin we assign to haloes with $\lambda > \lambda_{\text{crit}}(M_h)$ the type ‘‘spiral’’ and the type ‘‘elliptical’’ to haloes with $\lambda < \lambda_{\text{crit}}(M_h)$;
- (iii) we compute stellar masses for each halo using the SHMR of Rodríguez-Puebla et al. (2015) for the two galaxy populations;
- (iv) we bin again the entire population, but this time in stellar mass; in each bin we compute the fraction of spirals and ellipticals as determined by our guess function $\lambda_{\text{crit}}(M_h)$ and we compare the result to the observed distribution from Kelvin et al. (2014);
- (v) we update the guess $\lambda_{\text{crit}}(M_h)$, iterating the steps above, until a satisfactory match to the target $f_T(M_*)$ of Kelvin et al. (2014) is found.

With this procedure we have defined a model galaxy population for which the morphological type distribution is matched to the halo spin distribution consistently with the given SHMR. Now we use equation (9), with an arbitrary constant $f_j = 0.5$ for both galaxy type and mass, to predict the Fall relation.

We also tried with a different approach, that is, starting from a stellar mass distribution, in each stellar mass bin we assumed a log-normal λ distribution (for the dark matter) and we set λ_{crit} to be the $f_T(M_*)$ -th percentile of the distribution, where $f_T(M_*)$ is the Kelvin et al. (2014) type fraction in that stellar mass bin. The results that we now discuss are basically identical in these two procedures.

The right-hand panel of Figure 7 shows the comparison of this model with the observations of RF12. In this case the model provides a poor representation of the data in two respects. First, a pure spin-bias scenario, in which ellipticals/spirals form in low-/high- λ haloes at a given mass, can not account for the difference in the average j_* at a fixed stellar mass as a function of galaxy type. This is not surprising and can be understood if one considers that the scatter of the λ -distribution (~ 0.25 dex) is smaller than the systematic shift of the Fall relations of discs and ellipticals ($\sim 0.5 - 0.6$ dex, RF12). Second, the shape of the predicted $j_* - M_*$ relation is non-linear and it steepens at about the peak mass of f_* : this results in an inconsistency with the most massive discs and ellipticals ($\log M_*/M_\odot \gtrsim 11$). Hence we confirm previous claims (RF12) that a pure spin-bias scenario is not able to explain the systematic difference of the specific angular momentum of spirals and ellipticals of a given stellar mass, even when coupling it with state-of-the-art SHMR.

Even if we also take into account the fact that elliptical galaxies have typically stopped forming stars several Gyrs ago, when the specific angular momentum of the halo was smaller ($j_h(z) \propto (1+z)^{-1/2}$, see equation 4), we are still not able to explain all the discrepancy between the re-

lation for spirals and ellipticals in a spin-bias scenario. This is illustrated by the black arrow in the right-hand panel of Figure 7, which shows that even an extreme scenario, in which all ellipticals were already quenched at $z = 3$, would be at most marginally consistent with the observed shift in normalization with respect to the spirals⁴.

Note, also, that our model is extreme, for the transition between spirals and ellipticals is sharp and unlikely to be realistic. In the case of a smoother transition the two distributions would move closer and they would be even more inconsistent with the large systematic separation observed for the Fall relations of spirals and ellipticals.

A pure spin-bias scenario has been recently invoked to explain the formation of the so-called Ultra Diffuse Galaxies (UDGs, see van Dokkum et al. 2015), which are very faint and extended galaxies that are extreme outliers of the mass-size relation. At a given stellar mass, these systems have on average higher angular momentum than the bulk of the galaxy distribution (e.g. Leisman et al. 2017) and this has been related to them being formed in the high- λ tail of the halo distribution (Amorisco & Loeb 2016). However, this is not necessarily the case since for a given stellar mass, a galaxy with an higher-than-average retained fraction f_j would also have an high specific angular momentum j_* for its mass even if the dark matter halo has an average spin λ (see equation 9). This is also in agreement with results from recent cosmological simulations, in which the analogous of these galaxies tend to live in non-peculiar dark matter haloes (see e.g. Di Cintio et al. 2017). In these simulations stellar feedback prevents the collapse of low- j gas in the central regions and induces energy and angular momentum exchanges between the dark matter halo and the galaxy, which ends up having larger angular momentum with respect to other galaxies of similar mass.

5 SUMMARY AND CONCLUSIONS

In this contribution we have used analytic models in a standard Λ CDM framework to study the average retention of angular momentum of galaxies as a function of their mass and type. We did this by comparing the stellar specific angular momenta of galaxies on the empirical Fall relation with that of their dark matter haloes, hence constructing a *stellar-to-halo angular momentum relation*. The main improvements with respect to previous works are that we derive the retained fraction of angular momentum f_j by imposing consistency with both the empirical Fall relation and the SHMR and that we explore the dependence of the results on the adopted SHMR. The main results are the following:

- we confirm that f_j is smaller than unity for all galaxies and that, on average, late-type galaxies have larger fractions with respect to early-types (by about a factor 3 – 5) at any given mass;
- we find a significant dependence of f_j on stellar or halo mass for both morphological types and almost all SHMR,

⁴ Only modest deviations from the SHMR at $z = 0$ are expected for that at $z = 3$ in the stellar mass range relevant for ellipticals $M_* \gtrsim 10^{10} M_\odot$ (Behroozi, Wechsler, & Conroy 2013, e.g.). Hence, for simplicity, in this calculation we have used the SHMR at $z = 0$.

with the only exception of the Dutton et al. (2010) prescription for spirals, mostly due to the limited mass range considered there;

- we find that the $f_j - M_h$ relation is well represented by a double power-law model as in equation (18) and we provide the best fit parameters of the double power-law function for all the SHMR (Table 1);
- we infer a very conservative *upper limit* on the scatter of the $f_j - M_h$ relation of about 0.32 – 0.36 dex;
- we find that the ratio of stellar to halo angular momentum depends on the star formation efficiency roughly as $f_j \propto f_*^{2/3}$;
- we confirm that the spin-bias scenario (in which galaxies with different morphologies inhabit haloes with different spin) is not sufficient to explain the segregation of spirals and ellipticals in the $j_* - M_*$ plane;
- our results are consistent with a biased collapse scenario, in which $f_j \propto f_*^s$. The relatively low value $s \simeq 2/3$ required by the Fall relation is suggestive of mixing processes having altered the angular momentum distribution of baryons in the halo before or while a fraction f_*/f_b of them collapsed to form the central galaxy.

During the completion of this work, Shi et al. (2017) published a model of biased collapse to reproduce the Fall relation and the star formation efficiency. The main differences with our work are i) their best model predicts a significant flattening of the Fall relation for spirals at low masses, ii) they do their calculations for only one choice of the SHMR (relatively similar to the one by Dutton et al. 2010), iii) they try to disentangle a fraction f_{inf} of accreted material from a fraction f_j of retained angular momentum, based on metallicity evolution arguments. We refrained from (iii) due to the inherent uncertainties and degeneracy in the two parameters and, in fact, our f_j includes both processes and should be compared with their $f_j f_{\text{inf}}$.

ACKNOWLEDGEMENTS

LP thanks Emmanouil Papastergis and Crescenzo Tortora for many useful discussions. LP acknowledges financial support from a Vici grant from NWO. GP acknowledges support from the Swiss National Foundation grant PP00P2_163824. EDT acknowledges the support of the Australian Research Council (ARC) through grant DP160100723.

REFERENCES

- Aarseth S. J., Fall S. M., 1980, ApJ, 236, 43
 Amorisco N. C., Loeb A., 2016, MNRAS, 459, L51
 Barnes J. E., 1992, ApJ, 393, 484
 Barnes J., Efstathiou G., 1987, ApJ, 319, 575
 Behroozi P. S., Wechsler R. H., Conroy C., 2013, ApJ, 770, 57
 Binney, J., & Tremaine, S. 2008, Galactic Dynamics, 2nd edn. Princeton Univ. Press, Princeton, NJ
 Brook C. B., et al., 2011, MNRAS, 415, 1051
 Brook C. B., Stinson G., Gibson B. K., Roškar R., Wadsley J., Quinn T., 2012, MNRAS, 419, 771
 Bryan G. L., Norman M. L., 1998, ApJ, 495, 80
 Burkert A., et al., 2016, ApJ, 826, 214

- Chowdhury A., Chengalur J. N., 2017, *MNRAS*, 467, 3856
- Cortese L., et al., 2016, *MNRAS*, 463, 170
- Dalcanton J. J., Spergel D. N., Summers F. J., 1997, *ApJ*, 482, 659
- Davies R. L., Efstathiou G., Fall S. M., Illingworth G., Schechter P. L., 1983, *ApJ*, 266, 4
- DeFelippis D., Genel S., Bryan G. L., Fall S. M., 2017, *ApJ*, 841, 16
- Di Cintio A., Brook C. B., Dutton A. A., Macciò A. V., Obreja A., Dekel A., 2017, *MNRAS*, 466, L1
- Dutton A. A., Conroy C., van den Bosch F. C., Prada F., More S., 2010, *MNRAS*, 407, 2
- Dutton A. A., van den Bosch F. C., 2012, *MNRAS*, 421, 608
- Dutton A. A., Macciò A. V., 2014, *MNRAS*, 441, 3359
- Efstathiou G., Jones B. J. T., 1979, *MNRAS*, 186, 133
- El-Badry K., et al., 2017, *arXiv*, arXiv:1705.10321
- Fall S. M., 1983, *IAUS*, 100, 391
- Fall S. M., Efstathiou G., 1980, *MNRAS*, 193, 189
- Fall S. M., Romanowsky A. J., 2013, *ApJ*, 769, L26
- Ferrero I., et al., 2017, *MNRAS*, 464, 4736
- Fraternali F., Binney J. J., 2008, *MNRAS*, 386, 935
- Genel S., Fall S. M., Hernquist L., Vogelsberger M., Snyder G. F., Rodriguez-Gomez V., Sijacki D., Springel V., 2015, *ApJ*, 804, L40
- Governato F., Willman B., Mayer L., Brooks A., Stinson G., Valenzuela O., Wadsley J., Quinn T., 2007, *MNRAS*, 374, 1479
- Harrison, C. M. 2017, *Nature Astronomy*, 1, 0165
- Harrison C. M., et al., 2017, *arXiv*, arXiv:1701.05561
- Hernquist L., Mihos J. C., 1995, *ApJ*, 448, 41
- Hoyle F., 1949, Burgers J.M., van de Hulst H.C., eds., in *Problems of Cosmical Aerodynamics*, Central Air Documents Office, Dayton, p. 195
- Kassin S. A., Devriendt J., Fall S. M., de Jong R. S., Allgood B., Primack J. R., 2012, *MNRAS*, 424, 502
- Kauffmann G., Huang M.-L., Moran S., Heckman T. M., 2015, *MNRAS*, 451, 878
- Kelvin L. S., et al., 2014, *MNRAS*, 444, 1647
- Kravtsov A. V., 2013, *ApJ*, 764, L31
- Leauthaud, A., Tinker, J., Bundy, K., et al. 2012, *ApJ*, 744, 159
- Leisman, L., Haynes, M. P., Janowiecki, S., et al. 2017, *ApJ*, 842, 133
- Macciò A. V., Dutton A. A., van den Bosch F. C., Moore B., Potter D., Stadel J., 2007, *MNRAS*, 378, 55
- Miller S. H., Ellis R. S., Newman A. B., Benson A., 2014, *ApJ*, 782, 115
- Mo H. J., Mao S., White S. D. M., 1998, *MNRAS*, 295, 319
- Moster B. P., Naab T., White S. D. M., 2013, *MNRAS*, 428, 3121
- Navarro J. F., Frenk C. S., White S. D. M., 1996, *ApJ*, 462, 563
- Navarro J. F., Frenk C. S., White S. D. M., 1997, *ApJ*, 490, 493
- Navarro J. F., Steinmetz M., 2000, *ApJ*, 538, 477
- Obreschkow D., Glazebrook K., 2014, *ApJ*, 784, 26
- Pedrosa S. E., Tissera P. B., 2015, *A&A*, 584, A43
- Peebles P. J. E., 1969, *ApJ*, 155, 393
- Planck Collaboration, Ade, P. A. R., Aghanim, N., et al. 2016, *A&A*, 594, A13
- Porciani C., Dekel A., Hoffman Y., 2002, *MNRAS*, 332, 325
- Rodríguez-Puebla A., Avila-Reese V., Yang X., Foucaud S., Drory N., Jing Y. P., 2015, *ApJ*, 799, 130
- Romanowsky, A. J., & Fall, S. M. 2012, *ApJS*, 203, 17
- Rubin, V. C., Ford, W. K., Jr., & Thonnard, N. 1980, *ApJ*, 238, 471
- Shi, J., Lapi, A., Mancuso, C., Wang, H., & Danese, L. 2017, *arXiv:1706.02165*
- Somerville R. S., et al., 2008, *ApJ*, 672, 776-786
- Sokolowska A., Capelo P. R., Fall S. M., Mayer L., Shen S., Bonoli S., 2017, *ApJ*, 835, 289
- Stevens A. R. H., Croton D. J., Mutch S. J., 2016, *MNRAS*, 461, 859
- Teklu A. F., Remus R.-S., Dolag K., Beck A. M., Burkert A., Schmidt A. S., Schulze F., Steinborn L. K., 2015, *ApJ*, 812, 29
- Tinker J. L., et al., 2017, *ApJ*, 839, 121
- Tully R. B., Fisher J. R., 1977, *A&A*, 54, 661
- Vale A., Ostriker J. P., 2004, *MNRAS*, 353, 189
- van den Bosch F. C., 1998, *ApJ*, 507, 601
- van den Bosch F. C., Burkert A., Swaters, R. A. 2001, *MNRAS*, 326, 1205
- van Dokkum P. G., Abraham R., Merritt A., Zhang J., Geha M., Conroy C., 2015, *ApJ*, 798, L45
- van Uitert E., et al., 2016, *arXiv*, arXiv:1601.06791
- Veilleux S., Cecil G., Bland-Hawthorn J., 2005, *ARA&A*, 43, 769
- Yang X., Mo H. J., van den Bosch F. C., 2003, *MNRAS*, 339, 1057
- Zavala J., et al., 2016, *MNRAS*, 460, 4466

This paper has been typeset from a $\text{\TeX}/\text{\LaTeX}$ file prepared by the author.